The Version of Record of this manuscript has been published and is available in *Radiochimica Acta* **2022,** *110* (5), 291–300
26 April 2022 https://doi.org/10.1515/ract-2021-1134

Spectroscopic investigation of the different complexation and extraction properties of diastereomeric diglycolamide ligands

Patrik Weßling,*[a,b] Michael Trumm[b], Thomas Sittel,[a,b] Andreas Geist,[b] and Petra J. Panak[a,b]

[a]Karlsruhe Institute of Technology (KIT), Institute for Nuclear Waste Disposal (INE), P.O. Box 3640, 76021 Karlsruhe, Germany. E-mail: patrik.wessling@partner.kit.edu; Tel: +49 (0)721 60824652

[b]Heidelberg University, Institute for Physical Chemistry, Im Neuenheimer Feld 253, 69120 Heidelberg, Germany

Abstract

(2R,2'S)-2,2'-oxybis-(N,N-didecylpropanamide) (cis-mTDDGA) and (2R,2'R)-2,2'-oxybis-(N,N-didecylpropanamide) (trans-mTDDGA) were studied using time-resolved laser fluorescence spectroscopy (TRLFS), vibronic side-band spectroscopy (VSBS), and density functional theory calculations (DFT) to find reasons for their different extraction properties. Stability constants of the respective Cm(III) and Eu(III) complexes show cis-mTDDGA to be the superior ligand which is in agreement with results from extraction experiments. cis-mTDDGA extracts Cm(III) and Eu(III) as 1:3 complexes. In case of trans-mTDDGA, 1:2 complexes of the form $[M(\text{trans-mTDDGA})_2(\kappa^1\text{-}NO_3)(H_2O)_2]^{2+}$ (M = Cm, Eu) are extracted additionally to the 1:3 complexes. VSBS and DFT confirm the presence of inner-sphere nitrate in the 1:2 complex.

Keywords

Time-resolved laser fluorescence spectroscopy, curium, mTDDGA, diglycolamide, vibronic side-band spectroscopy, DFT, diastereomers

1 Introduction

Diglycolamides (DGA) are promising ligands for the extraction of actinides.[1-3] Several processes (e.g. DIAMEX, i-SANEX, ALSEP) for the separation of trivalent actinides (americium, curium) using 2,2'-oxybis*(N,N*-dioctylacetamide (TODGA) or 2,2'-oxybis*(N,N*-di-(2-ethylhexyl) acetamide (T2EHDGA) have been developed and tested on the laboratory scale.[4-8] These processes address the "heterogenous recycling" of irradiated nuclear fuels.[7, 9] Slightly different processes (e.g GANEX) are developed for "homogeneous" recycling routes,[9] co-separating the transuranium elements (neptunium, plutonium, americium, and curium). GANEX processes are generally comprised of two cycles: The 1st cycle separates uranium from dissolved spent nuclear fuel while the 2nd cycle separates the transuranium elements from the raffinate of the 1st cycle. To allow for sufficient plutonium loading in the 2nd cycle, the solvent (i. e. the organic phase) contains a mixture of TODGA and a second extracting agent, bis-(2-ethylhexyl) phosphoric acid (HDEHP)[10, 11] or *N,N'*-dimethyl-*N,N'*-dioctyl-2-(2-hexyloxy)ethyl)malonamide (DMDOHEMA),[12-14] dissolved in kerosene (see Scheme 1). However, adding a second extracting agent complicates process implementation, and should ideally be avoided.

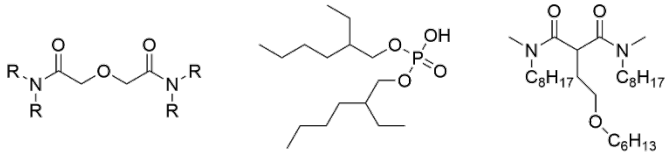

Scheme 1 TODGA (R = n-octyl) and T2EHDGA (R = 2-ethylhexyl), HDEHP (centre), DMDOHEMA (right).

The Version of Record of this manuscript has been published and is available in *Radiochimica Acta* **2022,** *110* (5), 291–300
26 April 2022 https://doi.org/10.1515/ract-2021-1134

Another way to increase plutonium loading capacity is increasing the TODGA concentration. This unfortunately results in increased co-extraction of unwanted species such as some fission products (e.g. Sr, Mo). To counteract, the TODGA molecule needs to be modified to obtain lower distribution ratios. Adding one or two methyl moieties (Scheme 2) progressively reduces the DGA's affinity for metal ions such as trivalent actinides and lanthanides. This was shown for both a lipophilic DGA[15] (i. e. an extracting agent, R = n-octyl) and a hydrophilic DGA (i. e. a masking agent,R = ethyl).[16]

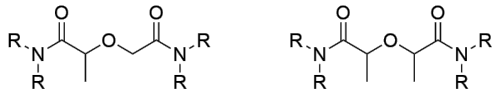

Scheme 2 Methylated (left) and bis-methylated (right) diglycolamides.

This concept was followed recently, together with replacing the n-octyl moieties by n-decyl: a solvent containing 0.5 mol L^{-1} 2,2'-oxybis-(N,N-didecylpropanamide) (mTDDGA, Scheme 2 right, R = n-decyl) in n-dodecane shows a plutonium loading capacity superior to that of the TODGA-HDEHP and TODGA-DMDOHEMA solvents. Also, the co-extraction of some fission products is less pronounced.[17]

mTDDGA exists in three isomeric forms (Scheme 3): the R,S or S,R (meso- or henceforth called "cis-mTDDGA"), the R,R isomer and the S,S isomer, the latter ones being enantiomers (henceforth called "trans-mTDDGA"). As already known for the n-octyl analogue,[18] cis-mTDDGA extracts trivalent actinide and lanthanide ions to a greater extent compared to trans-mTDDGA.[19] DFT calculations indicate that the cis diastereomer is the superior extracting agent due to the position of the nitrate in the extracted complex and its distance to the metal ion.[18]

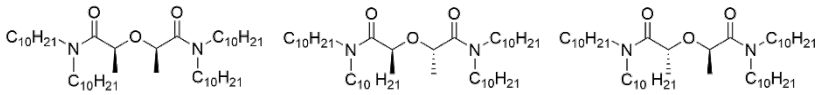

Scheme 3 meso- or cis-mTDDGA (left) and trans-mTDDGA (S,S-isomer, middle and R,R-isomer right).

To better understand the diastereomers' different extraction behaviour, the complexation of Cm(III) and Eu(III) (respectively representing trivalent actinide and lanthanide ions) with cis- and trans-mTDDGA was studied using time-resolved laser fluorescence spectroscopy (TRLFS). Fluorescence emission spectra of the complexes formed upon extraction of Cm(III) and Eu(III) from nitric acid solutions were compared to spectra obtained from monophasic titration experiments in propanol solutions. Additional insight was gained from vibronic side-band spectroscopy (VSBS) and quantum chemical calculations (DFT).

2 Experimental

2.1 Chemicals

All chemicals were used as purchased without further purification. cis-/trans-mTDDGA were synthetized analogue to literature procedure[20] and the diastereomers were separated by column chromatography (Silica, Petrolether:Diethylether (1:3)). In case of trans-mTDDGA, no separation of the R,R and S,S enantiomers was performed and neither identities or optical purities were determined. Hence, no statement about the enamtiomeric excess of the trans-mTDDGA solutions can be given.

2.2 Preparation of monophasic samples

For monophasic experiments in dependence of the ligand concentration 4.5 mg cis-mTDDGA or 118.2 mg trans-mTDDGA were dissolved in 2 mL (cis-mTDDGA) or 1 mL (trans-mTDDGA) of 2-propanol with 5 Vol.% H_2O and 1 x 10^{-2} mol L^{-1} $HClO_4$. If needed dilutions were prepared maintaining the solvent matrix. This solvent is chosen to ensure sufficient solubility of both Cm(III) and cis-/trans-mTDDGA.

For monophasic experiments in dependence of the nitrate concentration 0.97 g of Tetrabutylammonium nitrate (TBAN) were dissolved in 2 mL solutions containing 5.7 x 10^{-3} mol L^{-1} trans-mTDDGA or 1.1 x 10^{-3} mol L^{-1} cis-mTDDGA both in 2-propanol with 5 Vol.% H_2O and 1 x 10^{-2} mol L^{-1} $HClO_4$.
4.7 μL of 2.12 x 10^{-5} mol L^{-1} $Cm(ClO_4)_3$ or 9.4 μL of 1.07 x 10^{-3} mol L^{-1} $Eu(ClO_4)_3$ in 0.1 mol L^{-1} $HClO_4$ were dissolved with 995.3 μL or 990.6 μL of solvent resulting in initial Cm(III) or Eu(III) concentrations of 1 x 10^{-7} mol L^{-1} and 1 x 10^{-5} mol L^{-1}. Ligand concentrations were gradually increased by adding aliquots of the aforementioned solutions every 20 min. This time proved sufficient to attain chemical equilibrium.

2.3 Solvent extraction

Both Cm(III) and Eu(III) were extracted from HNO_3 with cis- and trans-mTDDGA. Organic phases were 0.5 mol L^{-1} cis- or trans-mTDDGA dissolved in kerosene (Exxsol D80). Aqueous phases were 1 x 10^{-7} mol L^{-1} Cm(III) or 1 x 10^{-5} mol L^{-1} Eu(III) in 5 mol L^{-1} HNO_3. 500 μL of each phase were shaken for 1 h at 298 K in a 2 mL screw-cap vial on an orbital vortex shaker (2500 rpm). After centrifugation (2 min, 6000 rpm) 300 μL of the organic phase were investigated by TRLFS and, in case of trans-mTDDGA, by VSBS.

2.4 TRLFS

TRLFS experiments were performed at 298 K with a Nd:YAG (Surelite II laser, Continuum) pumped dye laser system (NarrowScan D-R; Radiant Dyes Laser Accessories GmbH). A wavelength of 394.0 nm (Eu(III)) or 396.6 nm (Cm(III)) was used to excite the metal ions. Spectral decomposition was performed with a spectrograph (Shamrock 303i, ANDOR) with 1199 lines per mm gratings. The fluorescence was detected by an ICCD Camera (iStar Gen III, ANDOR). A delay of 1 μs was used to discriminate short-lived organic fluorescence and light scattering.

2.5 VSBS

Samples for VSBS contained 1 x 10^{-7} mol L^{-1} Cm(III) and either 1.4 x 10^{-2} mol L^{-1} trans-mTDDGA or 5.7 x 10^{-3} mol L^{-1} and 0.1 mol L^{-1} TBAN in 2-propanol with 5 Vol.% H_2O and 1 x 10^{-2} mol L^{-1} $HClO_4$. A third samples was prepared by extraction (see Solvent extraction).
To detect vibronic sidebands Cm(III) emission spectra were recorded in a wavelength range of 620 – 800 nm using a 1199 lines per mm grating. As the detection width of this grating is limited to 40 nm the central wavelength was shifted in 10 nm steps to scan the aforementioned wavelength range.

2.6 Theoretical model

Structural optimizations of trans-mTDDGA and the Cm(III)-trans-mTDDGA complexes as well as calculations of Gibbs energies and vibrational modes were performed employing density functional theory on the B3-LYP[21]/def2-TZVP[22] level using the TURBOMOLE[23] program package. The Cm(III) ion was described by an ECP60MWB[24] small-core pseudo potential. Electron correlation was added by Møller-Plesset perturbation theory (MP2).
For comparison with the VSB spectra atomic contributions to the vibrational modes were scaled by r^{-6}, where r denotes the atomic distance to the Cm(III) ion. Vibrational spectra were obtained using Gaussian line broadening on determined frequencies.

3 Results and discussion

3. 1 Complexation of Cm(III) with cis- and trans-mTDDGA

3.1.1 cis-mTDDGA. The complexation of Cm(III) with cis-mTDDGA was studied in 2-propanol with 5 Vol.% H_2O and 1 x 10^{-2} mol L^{-1} $HClO_4$. Fig. 1 shows the Cm(III) emission spectra resulting from the transition $^6D'_{7/2} \rightarrow {}^8S'_{7/2}$ with increasing ligand concentration.

The Version of Record of this manuscript has been published and is available in *Radiochimica Acta* **2022,** *110* (5), 291–300
26 April 2022 https://doi.org/10.1515/ract-2021-1134

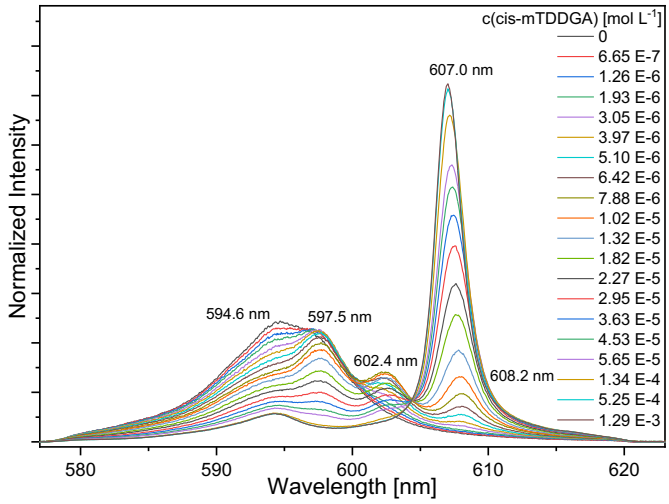

Fig. 1 Normalized Cm(III) emission spectra for the complexation of Cm(III) with cis-mTDDGA in 2-propanol with 5 Vol.% H_2O and 1 x 10^{-2} mol L^{-1} $HClO_4$ as a function of the cis-mTDDGA concentration ($c(Cm(III)_{ini}$ = 1 x 10^{-7} mol L^{-1}).

In absence of cis-mTDDGA the Cm(III) solvent spectrum has two emission bands at 594.6 nm and 597.5 nm resulting from different numbers of 2-propanol and water molecules in the first coordination sphere of Cm(III). The fluorescence lifetime is $\tau = 84 \pm 4$ μs (cf. SI, Fig S.1).

With increasing ligand concentration a bathochromic shift is observed in the Cm(III) emission spectra. The shift is caused by the increased ligand field splitting of the $^6D'_{7/2}$ state due to the complexation of Cm(III) with cis-mTDDGA. Three new emission bands at 597.5 nm, 602.4 nm and 608.2 nm are observed. The emission band at 608.2 nm shifts hypsochromically by 1.2 nm with increasing ligand concentration probably due to changes in the second coordination sphere of Cm(III). For ligand concentrations greater 5.3 x 10^{-4} mol L^{-1} an emission band at 607.0 nm and a hot band at 594.2 nm is observed. This spectrum is in good agreement with the emission spectrum of $[Cm(TODGA)_3]^{3+}$ in alcoholic solution[15] indicating the observed species to be the $[Cm(cis\text{-}mTDDGA)_3]^{3+}$ complex. The emission bands at 597.5 nm and 602.4 nm are assigned to the $[Cm(cis\text{-}mTDDGA)_n]^{3+}$ complexes (n = 1,2) by comparison with the respective Cm-TEDGA complexes.[16]

Using peak deconvolution and the relative fluorescence intensity (FI) factors (FI_1 = 1.5, FI_2 = 1.0 and FI_3 = 7.2, cf. SI, Fig. S2) the speciation of the $[Cm(cis\text{-}mTDDGA)_n]^{3+}$ complexes (n = 1-3) as a function of the free cis-mTDDGA concentration is obtained (Fig. 2) The FI factors denotes the fluorescence intensity of a given species in relation to a reference system – normally the solvent complex.

The Version of Record of this manuscript has been published and is available in *Radiochimica Acta* **2022,** *110* (5), 291–300
26 April 2022 https://doi.org/10.1515/ract-2021-1134

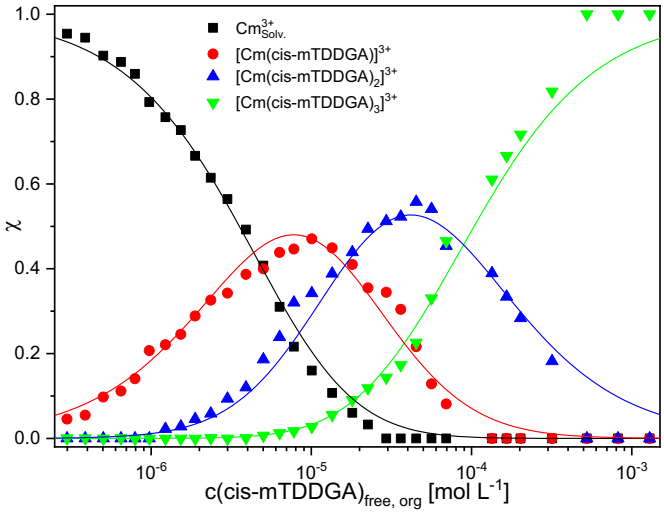

Fig. 2 Fractions of $[Cm(Solv.)]^{3+}$ and the $[Cm(cis\text{-}mTDDGA)_n]^{3+}$ complexes (n = 1-3) as a function of the free cis-mTDDGA concentration in 2-propanol with 5 Vol.% H_2O and 1 x 10^{-2} mol L^{-1} $HClO_4$. Symbols, experimental data. Lines, calculated with log β'_1 = 5.4, log β'_2 = 10.2 and log β'_3 = 14.2.

The 1:1 and 1:2 complexes form with maximum fractions of 48% and 56% at cis-mTDDGA concentrations of 1 x 10^{-5} mol L^{-1} and 5 × 10^{-5} mol L^{-1}, respectively. For cis-mTDDGA concentrations greater than 1 x 10^{-4} mol L^{-1} the 1:3 complex is the dominating species.

The proposed stoichiometries are confirmed by slope analyses according to eqn (1).

$$[ML_{n-1}]^{3+} + L \rightleftharpoons [ML_n]^{3+}$$

$$log\,\frac{c([ML_n]^{3+})}{c([ML_{n-1}]^{3+})} = log\ c(L) + logK'_n \quad (1)$$

Plotting log(c($[ML_n]^{3+}$)/c($[ML_{n-1}]^{3+}$)) vs. log(c(L)) yields slopes of m_1 = 1.07 ± 0.03, m_2 = 0.91 ± 0.05 and m_3 = 1.09 ± 0.05 (see Fig. S3), confirming the stepwise addition of one cis-mTDDGA molecule to form 1:1, 1:2 and 1:3 complexes.

Conditional stability constants are calculated according to eqn (2).

$$\beta'_n = \frac{c([ML_n]^{3+})}{c([M_{Solv.}]^{3+})(c(L))^n} \quad (2)$$

They are log β'_1 = 5.4 ± 0.2, log β'_2 = 10.2 ± 0.3 and log β'_3 = 14.2 ± 0.4

3.1.2 trans-mTDDGA. The complexation of Cm(III) with trans-mTDDGA was studied analogously. The Cm(III) emission spectra are shown in Fig. S4.

In line with the complexation of Cm(III) with cis-mTDDGA, three emission bands at 597.5 nm, 602.2 nm and 608.4 nm (shifting to 607.9 nm upon further addition of ligand) are observed. The emission bands are assigned to the $[Cm(trans\text{-}mTDDGA)_n]^{3+}$ complexes (n = 1-3).

The species distribution as a function of the free ligand concentration (Fig. S5) is obtained by peak deconvolution using the following FI factors: FI_1 = 1.5, FI_2 = 1.0 and FI_3 = 5.2 (cf. SI, Fig. S6).

The stoichiometries are confirmed by slope analyses (see SI, Tab. S1 and Fig. S7). Stability constants are log β'_1 = 4.8 ± 0.2, log β'_2 = 9.5 ± 0.3 and log β'_3 = 13.1 ± 0.3.

The Version of Record of this manuscript has been published and is available in *Radiochimica Acta* **2022,** *110* (5), 291–300
26 April 2022 https://doi.org/10.1515/ract-2021-1134

3.2 Complexation of Eu(III) with cis- and trans-mTDDGA

Furthermore, the complexation of Eu(III) with cis- and trans-mTDDGA in 2-propanol with 5 Vol.% H_2O and 1 x 10^{-2} mol L^{-1} was studied. The fluorescence spectra resulting from the transition $^5D_0 \rightarrow {}^7F_n$ (n = 1,2) for the complexation of Eu(III) with cis- or trans-mTDDGA as a function of the mTDDGA concentrations are given in Fig. 3 (left) and Fig. S8.

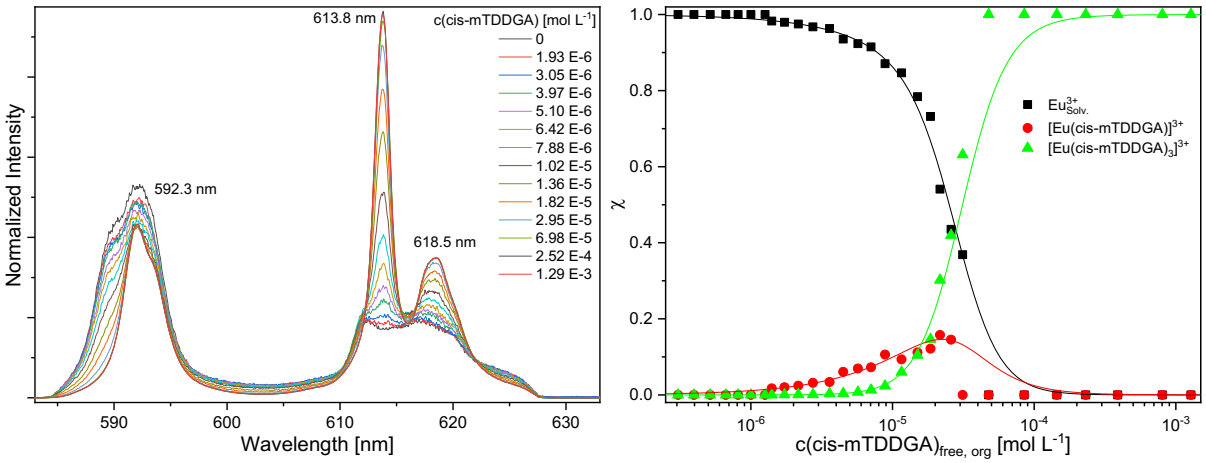

Fig. 3 Left: Normalized Eu(III) emission spectra for the complexation of Eu(III) with cis-mTDDGA (right) in 2-propanol + 5 Vol.% H_2O and 1 x 10^{-2} mol L^{-1} $HClO_4$ as a function of the cis-mTDDGA concentration ($c(Eu(III)_{ini}$ = 1 x 10^{-5} mol L^{-1}). Right: Fractions of $[Eu(Solv.)]^{3+}$ and the $[Eu(cis\text{-}mTDDGA)_n]^{3+}$ complexes (n = 1,3) as a function of the free cis-mTDDGA concentration in 2-propanol + 5 Vol.% H_2O and 1 x 10^{-2} mol L^{-1} $HClO_4$. Dots, experimental data. Lines, calculated for cis-mTDDGA with $\log\beta'_1$ = 4.1 and $\log\beta'_3$ = 13.7.

Without addition of the ligands the Eu(III) solvent spectrum is observed. It is characterized by an intensive $^7F_1$ emission band at 592.3 nm with a shoulder at 590.0 nm and a comparably small $^7F_2$ emission band with maxima at 612.4 and 617.4 nm. The fluorescence lifetime is τ = 135 ± 7 μs (cf. SI, Fig S1). The addition of cis-/trans-mTDDGA leads to a strong increase in intensity and a splitting of the $^7F_2$ emission bands. No further changes in the Eu(III) emission spectra are observed for concentrations greater 2.5 x 10^{-4} mol L^{-1} cis-mTDDGA or 1 x 10^{-3} mol L^{-1} trans-mTDDGA.

In line with the complexation of Cm(III), emission spectra at the highest ligand concentration are assigned to the Eu(III) 1:3 complexes. A further species occurring only in small amounts is identified to be the Eu(III) 1:1 complex (see below) with cis- or trans-mTDDGA. In contrast to the complexation of Cm(III) with cis- and trans-mTDDGA no spectroscopic evidence for a 1:2 complex with cis- or trans-mTDDGA with Eu(III) could be found

To obtain a speciation diagram peak deconvolution was performed taking the following FI factors (cf. SI, Fig. S9) FI_1 = 3 and FI_3 = 33 for cis-mTDDGA and FI_1 = 2 and FI_3 = 30 for trans-mTDDGA into account. The corresponding speciation diagrams are shown in Fig. 3 (right) and Fig. S10.

The 1:3 complex is observed for cis-mTDDGA concentrations greater than 5.9 x 10^{-6} mol L^{-1} and is the dominant species in the system for concentrations greater 3.1 x 10^{-5} mol L^{-1}. Approximately one order of magnitude higher ligand concentrations are required to form the corresponding trans-mTDDGA complexes.

Slope analyses (cf. Fig. S11 and Tab. S1) according to eqn (3) verified the observed species to be 1:1 and 1:3 complexes.

$$log\frac{c([EuL_n]^{3+})}{c([\mathrm{Eu(Solv.)}]^{3+})} = \mathrm{n} * log\ c(L) + log\beta'_n \quad (3)$$

Stability constants are given in Tab. 1.

The Version of Record of this manuscript has been published and is available in *Radiochimica Acta* **2022,** *110* (5), 291–300
26 April 2022 https://doi.org/10.1515/ract-2021-1134

3.3 Comparison of the derived stability constants

The stability constants for the complexation of Cm(III) and Eu(III) with cis- and trans-mTDDGA are summarized in Tab. 1.

For the complexation of both Cm(III) and Eu(III) higher stability constants are found for cis-mTDDGA. In comparison, the log β'_3 values for the complexation with cis-mTDDGA are 1.1 (for Cm(III)) and 1.8 (for Eu(III)) orders of magnitude higher than for the complexation with trans-mTDDGA, confirming cis-mTDDGA to be the stronger ligand.

Tab. 1 Stability constants log β'_n for the complexation of Cm(III) and Eu(III) with cis- and trans-mTDDGA in 2-propanol with 5 Vol.% H_2O and 1 x 10^{-2} mol L^{-1} $HClO_4$.

	n	Cm(III)	Eu(III)
cis-mTDDGA	1	5.4 ± 0.2	4.1 ± 0.2
	2	10.2 ± 0.3	-
	3	14.2 ± 0.4	13.7 ± 0.4
trans-mTDDGA	1	4.8 ± 0.2	3.9 ± 0.2
	2	9.5 ± 0.3	-
	3	13.1 ± 0.3	11.9 ± 0.4

The stability constants show that the stereoisomerism of the ligand influences its complexation properties. Similar observations are reported for the complexation of Eu(III) and Am(III) with tris-(2-pyridylmethyl)amine[25] or Pu(IV) with dicyclohexano-18-crown-6 ether.[26]

3.4 Solvent extraction

To determine the speciation under extraction conditions and obtain information on the differing extraction performance, extraction experiments were performed with both diastereomers. The organic phases (0.5 mol L^{-1} cis-/trans-mTDDGA in kerosene (Exxsol D80)) were investigated after extraction using TRLFS. Fig. 4 compares the normalized Cm(III) and Eu(III) emission spectra of the post-extraction organic phases to the emission spectra of the 1:3 complexes from the monophasic experiments.

With cis-mTDDGA, the post-extraction emission spectra (black lines) and the emission spectra of the 1:3 complexes (blue lines) are in good agreement, with small deviations caused by the different diluents. This confirms that both Cm(III) and Eu(III) are extracted as $[M(\text{cis-mTDDGA})_3](NO_3)_3$ complexes.

With trans-mTDDGA, distinct differences are observed between the post-extraction emission spectra (red lines) and the emission spectra of the 1:3 complexes (green lines). In case of Cm(III), an emission band with a maximum at 607.9 nm, a shoulder at 606.0 nm, and a hotband at 598.1 nm is observed in the post-extraction spectrum. For Eu(III), the spectrum displays the $^7F_1$ emission band at 592.2 nm and the $^7F_2$ emission band with maxima at 613.8 nm and 616.4 n. This indicates that in case of trans-mTDDGA a mixture of several Cm(III) and Eu(III) species are extracted.

Comparison with the Cm(III) emission spectra in 2-propanol with 5 Vol.% H_2O and 1 x 10^{-2} mol L^{-1} $HClO_4$ (see Fig. S4) indicates the 1:3 complex to be the major species. What is interesting, the shoulder at 606.0 nm does not result from the presence of the 1:2 complex (having its emission maximum at 602.2 nm, see Fig. S4). Therefore, it seems likely that in case of the extraction of Cm(III) from HNO_3, a ternary 1:2 complex, $[Cm(\text{trans-mTDDGA})_2(NO_3)_n(H_2O)_m](NO_3)_{(3-n)}$ is formed.

The Version of Record of this manuscript has been published and is available in *Radiochimica Acta* **2022,** *110* (5), 291–300
26 April 2022 https://doi.org/10.1515/ract-2021-1134

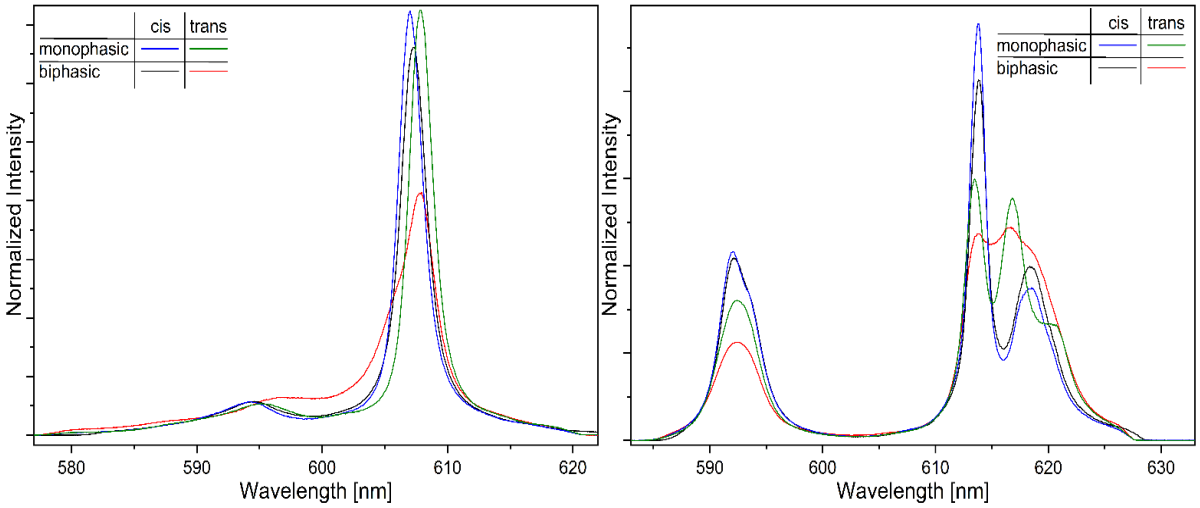

Fig. 4 Comparison of the normalized Cm(III) (left) and Eu(III) (right) emission spectra of the organic phases after the extraction (biphasic) and the emission spectra of the $[ML_3]^{3+}$ complexes (M = Cm, Eu; L = cis-/trans-mTDDGA) in 2-propanol with 5 Vol.% H_2O and 1 x 10^{-2} mol L^{-1} $HClO_4$ (monophasic). Biphasic: Organic phase: 0.5 mol L^{-1} cis-/trans-mTDDGA in kerosene (Exxsol D80). Aqueous phase: 1 x 10^{-7} mol L^{-1} Cm(III) or 1 x 10^{-5} mol L^{-1} Eu(III) in 5 mol L^{-1} HNO_3. A/O = 1; t = 1 h, T = 293 K. Monophasic: c(cis-mTDDGA) = 1.3 x 10^{-3} mol L^{-1} (Cm(III), Eu(III)); c(trans-mTDDGA) = 1.4 x 10^{-2} mol L^{-1} (Cm(III)) or 2.3 x 10^{-3} mol L^{-1} (Eu(III)); $c(Cm(III)_{ini})$ = 1 x 10^{-7} mol L^{-1}; $c(Eu(III)_{ini})$ = 1 x 10^{-5} mol L^{-1}.

3.5 Influence of the nitrate concentration

To verify the formation of a ternary complex, tetrabutylammonium nitrate (TBAN) was gradually added to a sample containing the $[Cm(trans\text{-}mTDDGA)_3]^{3+}$ complex in 2-propanol with 5 vol.% H_2O and 10^{-2} mol L^{-1} $HClO_4$. The trans-mTDDGA concentration was kept constant. The resulting Cm(III) emission spectra are shown in Fig. 5.

In absence of TBAN, the emission spectrum of the $[Cm(trans\text{-}mTDDGA)_3]^{3+}$ complex is observed (λ_{max} = 607.9 nm, $\lambda_{hotband}$ = 594.9 nm). Upon addition of TBAN a hypsochromic shift and a broadening of the emission band occurs. The continuous shift of the emission band in dependence of the nitrate concentration proofs the coordination of nitrate in the inner coordination sphere of Cm(III).

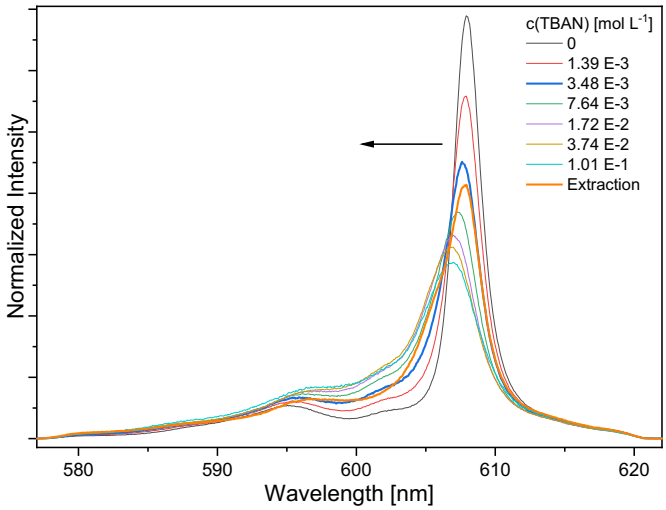

Fig. 5 Normalized Cm(III) emission spectra with 5.7 x 10^{-3} mol L^{-1} trans-mTDDGA in 2-propanol + 5 Vol.% H_2O and 1 x 10^{-2} mol L^{-1} $HClO_4$ as a function of the TBAN concentration and Cm(III) emission spectrum in the organic phase after extraction with 0.5 mol L^{-1} trans-mTDDGA from 5 mol L^{-1} HNO_3. ($c(Cm(III)_{ini}$ = 1 x 10^{-7} mol L^{-1}).

Fig. 5 also shows the emission spectrum of Cm(III) in the organic phase. A good agreement with the emission spectrum at 3.48×10^{-3} mol L^{-1} TBAN is observed. This supports the formation of a ternary 1:2 complex $[Cm(trans\text{-}mTDDGA)_2(NO_3)_n(H_2O)_m]^{(3-n)+}$ under extraction conditions.

Analogue experiments in dependence of the nitrate concentration were performed for Eu(III) with trans-mTDDGA as well as Cm(III) and Eu(III) with cis-mTDDGA. The fluorescence spectra are given in the SI in Fig. S12 – S14. Both the $^7F_0$ emission bands of Eu(III) with cis- and trans-mTDDGA and the Cm(III) emission band with cis-mTDDGA shift hypsochromically upon addition of TBAN, indiciating the presence of a ternary 1:2 complex. However, in case of cis-mTDDGA, higher TBAN concentrations are required to produce a shift similar to that with trans-mTDDGA. This is in good agreement with the higher stability constants for the complexation of Cm(III) and Eu(III) with cis-mTDDGA in comparison to the complexation with trans-mTDDGA. Therefore, cis-mTDDGA is a stronger competitor for nitrate resulting in higher amounts of nitrate needed to replace one of the ligands (cf. Tab. 1).

In case of Eu(III) a vibronic side band is observed at 742 cm^{-1} for both trans- and cis-mTDDGA. In agreement with the literature,[27-29] this vibronic side band originates from a nitrate anion coordinated in the first coordination sphere of Eu(III). As vibronic side bands can only be observed by TRLFS if the vibrating functional groups are coordinated directly to the probed metal, this further supports the replacement of a ligand molecule in the 1:3 complex by nitrate, thus forming a ternary 1:2 complex.

To identify the number of water molecules in the first coordination sphere of the ternary 1:2 complex the fluorescence lifetime at a TBAN concentration of 0.1 mol L^{-1} was determined. The measured Cm(III) fluorescence lifetime is $\tau = 289 \pm 21$ μs correlating with 1.4 molecules of water.[25] This proofs the presence of one or two molecules of water in the first coordination sphere of Cm(III).

DGA are tridentate ligand, occupying six coordination sites in the Cm(III) and Eu(III) 1:2 complexes. The remaining three sites are occupied by either water or nitrate molecules. Consequently, the fluorescence lifetimes are in agreement with the following three complexes:

- $[ML_2(\eta^2\text{-}NO_3)(H_2O)]^{2+}$
- $[ML_2(\eta^1\text{-}NO_3)_2(H_2O)]^{+}$
- $[ML_2(\eta^1\text{-}NO_3)(H_2O)_2]^{2+}$

The Version of Record of this manuscript has been published and is available in *Radiochimica Acta* **2022,** *110* (5), 291–300
26 April 2022 https://doi.org/10.1515/ract-2021-1134

3.6 Computational results

The mentioned ternary complexes were optimized using DFT to identify the energetically most stable one. The $[CmL_2(\eta^1\text{-}NO_3)(H_2O)_2]^{2+}$ complex (L = trans-mTDDGA) was optimized with three different arrangements of the nitrate and water molecules, see Fig. 6 (for the other two complexes, see Fig. S15). Reaction enthalpies are negative for all structures. Energies relative to the energetically most stable one are given in Tab. 2.

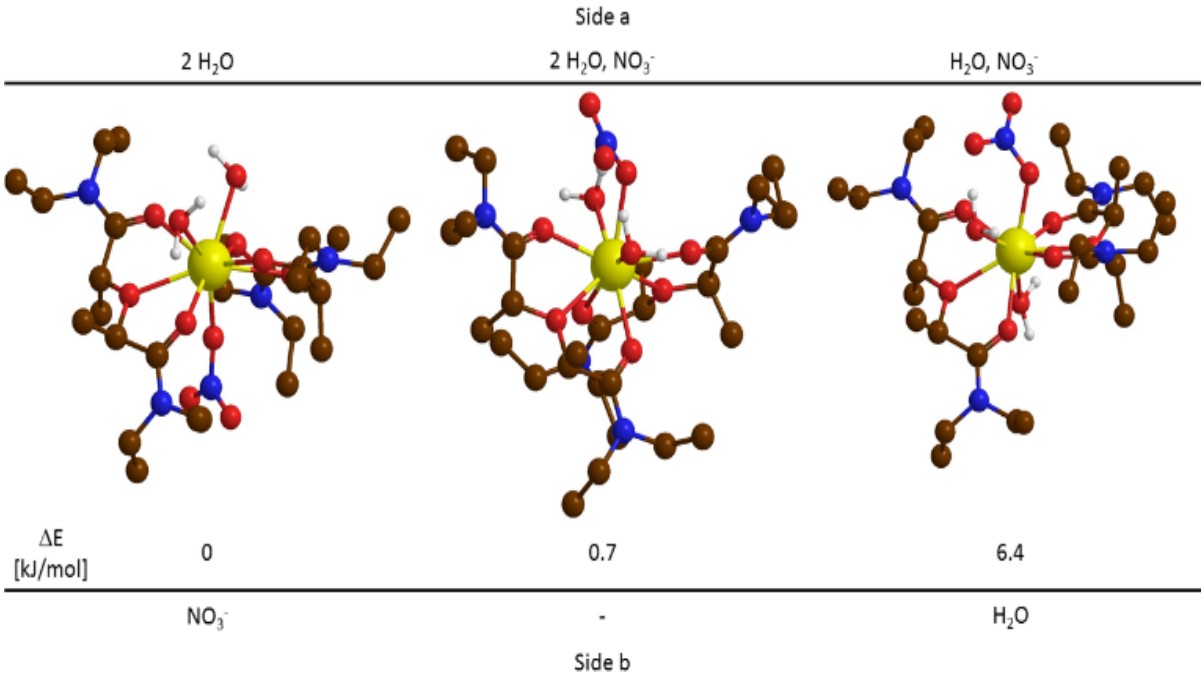

Fig. 6 Optimized structures of the [Cm(trans-mTDDGA)2(κ1-NO3)(H2O)2]2+ complexes with different arrangement of the water and nitrate molecules. Protons of the ligand framework are not shown. Carbon (brown), nitrogen (blue), oxygen (red), hydrogen (white), curium (yellow). Theoretical level: B3-LYP/def2-TZVP.

Tab. 2 Energy differences between the optimized structures of the $[CmL_2(NO_3)_n(H_2O)_m]^{(3-n)+}$ complexes in relation to the energetically most stable one. Theoretical level: B3-LYP/def2-TZVP.

Stoichiometry	Side a	Side b	ΔE [kJ mol^{-1}]
$[Cm(trans\text{-}mTDDGA)_2(\eta^1\text{-}NO_3)(H_2O)_2]^{2+}$	2 H_2O	NO_3^-	0
	2 H_2O, NO_3^-	-	0.7
	H_2O, NO_3^-	H_2O	6.4
$[Cm(trans\text{-}mTDDGA)_2(\eta^2\text{-}NO_3)(H_2O)]^{2+}$	NO_3^-	H_2O	50.1
$[Cm(trans\text{-}mTDDGA)_2(\eta^1\text{-}NO_3)_2(H_2O)_2]^{+}$	H_2O, NO_3^-	NO_3^-	108.8

The energetically most stable structure is $[CmL_2(\eta^1\text{-}NO_3)(H_2O)_2]^{2+}$ with the two water molecules on one side and the nitrate anion on the other side. Other arrangements of the water and nitrate molecules result in higher energies by 0.7–6.4 kJ mol^{-1}. Thus, the arrangement of the water and nitrate molecules does not have a significant influence, and therefore, an unambiguous conclusion as to their arrangement cannot be drawn from the results of DFT calculations.

In contrast, $[CmL_2(\eta^2\text{-}NO_3)(H_2O)]^{2+}$ is disfavoured by 50.1 kJ mol^{-1}, $[CmL_2(\eta^1\text{-}NO_3)_2(H_2O)_2]^{+}$ by 108.8 kJ mol^{-1}, ruling out their formation.

The Version of Record of this manuscript has been published and is available in *Radiochimica Acta* **2022,** *110* (5), 291–300
26 April 2022 https://doi.org/10.1515/ract-2021-1134

3.7 Vibronic side-band spectroscopy (VSBS)

Vibronic sideband spectroscopy (VSBS).[30, 31] was used to verify the inner-sphere coordinated nitrate molecule in the ternary 1:2 complex. This technique allows the observation of vibrations caused by functional groups directly coordinated to the probed metal ion. The recorded spectra consist of the zero phonon line (ZPL) and the side bands. Whereas the ZPL results from the electronic transition — in case of Cm(III) from the $^6D'_{7/2} \rightarrow {}^8S'_{7/2}$ transition— the vibronic side bands originate from changes in the dipole moment of the ligand field due to internal vibrations caused by the excitation of the probed metal ion. The energy of a vibration is given by eqn (4)

$$E(vibration) = E(ZPL) - E(vibronic\ sideband) (4)$$

Three samples were studied by VSBS:

1. Absence of nitrate: Cm(III) in 1.4 x 10^{-2} mol L^{-1} trans-mTDDGA in 2-propanol with 5 Vol.% H_2O and 1 x 10^{-2} mol L^{-1} $HClO_4$
2. Presence of nitrate: Cm(III) in 5.7 x 10^{-3} mol L^{-1} trans-mTDDGA and 0.1 mol L^{-1} TBAN in 2-propanol with 5 Vol.% H_2O and 10^{-2} mol L^{-1} $HClO_4$
3. Organic phase after extraction: Cm(III) extracted from 5 mol L^{-1} HNO_3 with 0.5 mol L^{-1} trans-mTDDGA dissolved in kerosene (Exxsol D80)

Due to the presence of the nitrate anion the vibronic side-band spectra of samples 2 and 3 are expected to differ from the side-band spectrum of sample 1 which exclusively contains the 1:3 complex. The vibronic side-band spectra are shown in Fig. 7.

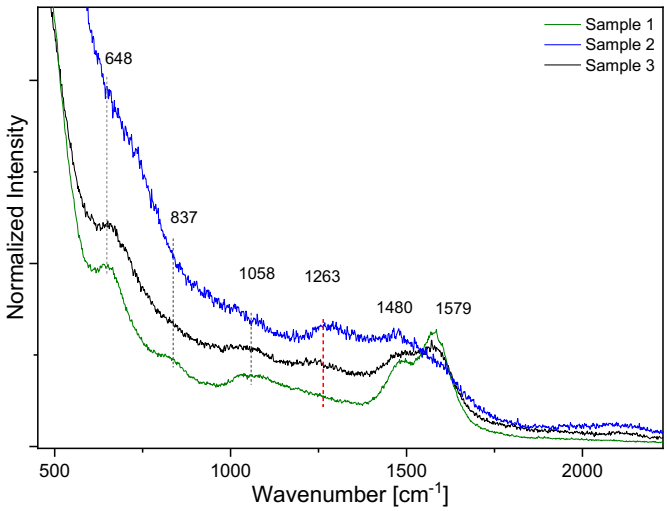

Fig. 7 Comparison of the experimental vibronic side bands of sample 1-3.

The three spectra show many similarities, e.g. the side bands at 648 cm^{-1}, 837 cm^{-1}, 1058 cm^{-1}, 1480 cm^{-1} and 1579 cm^{-1}. However, the vibronic side band at 1263 cm^{-1} is only found in presence of nitrate (sample 2) and in the organic phase after extraction (sample 3). As these two samples contain certain amounts of the 1:2 complex, the observed side bands confirm the presence of an inner-sphere nitrate anion in the ternary 1:2 complex.

Vibronic side bands were calculated for the three optimized structures of $[Cm(trans\text{-}mTDDGA)_2(\eta^1\text{-}NO_3)(H_2O)_2]^{2+}$ to assign the experimental vibronic side bands. The calculated vibronic side-band spectra are compared to the experimental spectrum of sample 2 in Fig. 8.

The Version of Record of this manuscript has been published and is available in *Radiochimica Acta* **2022,** *110* (5), 291–300
26 April 2022 https://doi.org/10.1515/ract-2021-1134

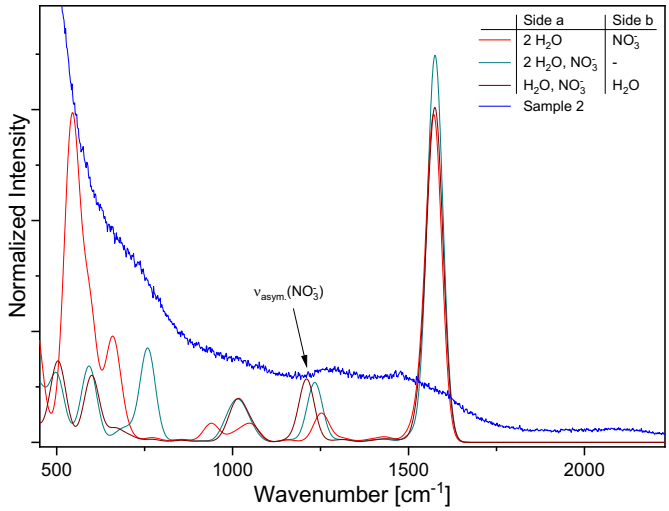

Fig. 8 Comparison of the calculated vibronic sidebands of the three structures of $[Cm(trans\text{-}mTDDGA)_2(NO_3)(H_2O)_2]^{2+}$ with the experimental vibronic sideband of Cm(III) in sample 2. $C(Cm(III)_{ini}) = 1 \times 10^{-7}$ mol L^{-1}.

The calculated vibronic side-band spectra are in good agreement with the experimental spectrum. Note that intensities cannot be calculated by the methods used. The calculated vibronic side bands allow assigning the experimental vibrational modes: vibrational modes at 648 cm^{-1}, 837 cm^{-1} and 1058 cm^{-1} are assigned to vibrational modes of the ligand framework while vibrational modes at 1480 cm^{-1} and 1579 cm^{-1} are attributed to the stretching mode of the coordinating carbonyl groups. The vibrational mode at 1263 cm^{-1} is assigned to the asymmetric stretching mode of the coordinated nitrate. The symmetric stretching mode and the bending modes of the nitrate are superimposed by the ZPL. Still, VSBS further strengthens the argument of the formation of a ternary 1:2 complex with nitrate and trans-mTDDGA.

4 Conclusions

To explain the differences in extraction performance between the diastereomers cis- and trans-mTDDGA, their complexation with Cm(III) and Eu(III) was studied using TRLFS, VSBS and DFT.

cis-mTDDGA is the superior ligand for both Cm(III) and Eu(III) ($\log \beta'_{3,Cm} = 14.2 \pm 0.4$, $\log \beta'_{3,Eu} = 13.7 \pm 0.4$) compared to trans-mTDDGA ($\log \beta'_{3,Cm} = 13.1 \pm 0.3$, $\log \beta'_{3,Eu} = 11.9 \pm 0.4$). Probing the organic phases after extraction verified Cm(III) and Eu(III) to be extracted as 1:3 complexes with cis-mTDDGA. However, in case of trans-mTDDGA a mixture of 1:3 and 1:2 complexes is found in the organic phase. The 1:2 complex is a ternary species, $[Cm(trans\text{-}mTDDGA)_2(NO_3)_n(H_2O)_m]^{(3-n)+}$. Fluorescence lifetime measurements and DFT calculations show that $[Cm(trans\text{-}mTDDGA)_2(\eta^1\text{-}NO_3)(H_2O)_2]^{2+}$ is the most stable structure in solution. The presence of an inner-sphere nitrate anion was verified by VSBS.

Conflicts of interest

There are no conflicts to declare.

Author contribution

All authors have accepted responsibility for the entire content of this submitted manuscript and approved submission.

Acknowledgements

This work has received funding from the European Research Council (ERC) under the European Union's Horizon 2020 research and innovation program (project GENIORS, grant agreement No. 755171) and the German Federal Ministry for Research and Education (grant agreement No. 02NUK059A, 02NUK059C).

Notes and references

1. Sasaki, Y., Sugo, Y., Suzuki, S., and Tachimori, S. The novel extractants, diglycolamides, for the extraction of lanthanides and actinides in HNO_3/*n*-dodecane system *Solvent Extr. Ion Exch.* 2001, *19,* 91.
2. Ansari, S.A., Pathak, P., Mohapatra, P.K., and Manchanda, V.K. Chemistry of diglycolamides: promising extractants for actinide partitioning *Chem. Rev.* 2012, *112,* 1751.
3. Whittaker, D., Geist, A., Modolo, G., Taylor, R., Sarsfield, M., and Wilden, A. Applications of diglycolamide based solvent extraction processes in spent nuclear fuel reprocessing, part 1: TODGA *Solvent Extr. Ion Exc.* 2018, *36,* 223.
4. Taylor, R. (ed.), *Reprocessing and Recycling of Spent Nuclear Fuel*. 2015, Cambridge, UK: Woodhead Publishing.
5. Bhattacharyya, A. and Mohapatra, P.K. Separation of trivalent actinides and lanthanides using various 'N', 'S' and mixed 'N,O' donor ligands: a review *Radiochim. Acta* 2019, *107,* 931.
6. Baron, P., Cornet, S.M., Collins, E.D., DeAngelis, G., Del Cul, G., Fedorov, Y., Glatz, J.P., Ignatiev, V., Inoue, T., Khaperskaya, A., Kim, I.T., Kormilitsyn, M., Koyama, T., Law, J.D., Lee, H.S., Minato, K., Morita, Y., Uhlíř, J., Warin, D., and Taylor, R.J. A review of separation processes proposed for advanced fuel cycles based on technology readiness level assessments *Progr. Nucl. Energy* 2019, *117,* 103091.
7. Geist, A., Adnet, J.-M., Bourg, S., Ekberg, C., Galán, H., Guilbaud, P., Miguirditchian, M., Modolo, G., Rhodes, C., and Taylor, R. An overview of solvent extraction processes developed in Europe for advanced nuclear fuel recycling, part 1 — heterogeneous recycling *Separ. Sci. Technol.* 2021, *56,* 1866.
8. Wilden, A., Kreft, F., Schneider, D., Paparigas, Z., Modolo, G., Lumetta, G.J., Gelis, A.V., Law, J.D., and Geist, A. Counter current actinide lanthanide separation process (ALSEP) demonstration test with a simulated PUREX raffinate in centrifugal contactors on the laboratory scale *Applied Sciences* 2020, *10,* 7217.
9. OECD-NEA, *Homogeneous versus heterogeneous recycling of transuranics in fast nuclear reactors*, in *NEA No. 7077*. 2012, Nuclear Energy Agency (NEA), Paris.
10. Miguirditchian, M., Chareyre, L., Hérès, X., Hill, C., Baron, P., and Masson, M., *GANEX: adaptation of the DIAMEX-SANEX process for the group actinide separation*, in *Proc. Internat. Conf. GLOBAL 2007 (Advanced Nuclear Fuel Cycles and Systems)*. 2007: Boise, Idaho, USA, 9–13 September 2007.
11. Miguirditchian, M., Roussel, H., Chareyre, L., Baron, P., Espinoux, D., Calor, J.-N., Viallesoubranne, C., Lorrain, B., and Masson, M., *HA demonstration in the Atalante facility of the GANEX 2nd cycle for the grouped TRU extraction*, in *Proc. Internat. Conf. GLOBAL 2009 (The Nuclear Fuel Cycle: Sustainable Options & Industrial Perspectives)*. 2009: Paris, France, 6–11 September.
12. Carrott, M., Geist, A., Hérès, X., Lange, S., Malmbeck, R., Miguirditchian, M., Modolo, G., Wilden, A., and Taylor, R. Distribution of plutonium, americium and interfering fission products between nitric acid and a mixed organic phase of TODGA and DMDOHEMA in kerosene, and implications for the design of the "EURO-GANEX" process *Hydrometallurgy* 2015, *152,* 139.
13. Carrott, M., Bell, K., Brown, J., Geist, A., Gregson, C., Hérès, X., Maher, C., Malmbeck, R., Mason, C., Modolo, G., Müllich, U., Sarsfield, M., Wilden, A., and Taylor, R. Development of a new flowsheet for co-separating the transuranic actinides: the "EURO-GANEX" process *Solvent Extr. Ion Exch.* 2014, *32,* 447.
14. Malmbeck, R., Magnusson, D., Bourg, S., Carrott, M., Geist, A., Hérès, X., Miguirditchian, M., Modolo, G., Müllich, U., Sorel, C., Taylor, R., and Wilden, A. Homogenous recycling of transuranium elements from irradiated fast reactor fuel by the EURO-GANEX solvent extraction process *Radiochim. Acta* 2019, *107,* 917.
15. Wilden, A., Modolo, G., Lange, S., Sadowski, F., Beele, B.B., Skerencak-Frech, A., Panak, P.J., Iqbal, M., Verboom, W., Geist, A., and Bosbach, D. Modified diglycolamides for the An(III) + Ln(III) co-separation: evaluation by solvent extraction and time-resolved laser fluorescence spectroscopy *Solvent Extr. Ion Exch.* 2014, *32,* 119.
16. Klaß, L., Wilden, A., Kreft, F., Wagner, C., Geist, A., Panak, P.J., Herdzik-Koniecko, I., Narbutt, J., and Modolo, G. Evaluation of the hydrophilic complexant *N,N,N',N'*-tetraethyldiglycolamide (TEDGA) and its methyl-substituted analogues in the selective Am(III) separation *Solvent Extr. Ion Exch.* 2019, *37,* 297.
17. Malmbeck, R., Magnusson, D., and Geist, A. Modified diglycolamides for grouped actinide separation *J. Radioanal. Nucl. Chem.* 2017, *314,* 2531.
18. Wilden, A., Kowalski, P.M., Klaß, L., Kraus, B., Kreft, F., Modolo, G., Li, Y., Rothe, J., Dardenne, K., Geist, A., Leoncini, A., Huskens, J., and Verboom, W. Unprecedented inversion of selectivity and extraordinary difference in the complexation of trivalent f-elements by diastereomers of a methylated diglycolamide *Chem. Eur. J.* 2019, *25,* 5507.

19. Verlinden, B., Wilden, A., Van Hecke, K., Egberink, R.J.M., Huskens, J., Verboom, W., Hupert, M., Weßling, P., Geist, A., Panak, P.J., Hermans, R., Verwerft, M., Modolo, G., Binnemanns, K., Cardineals, T. *Solvent Extr. Ion Exch. (submitted)*.
20. Iqbal, M., Huskens, J., Verboom, W., Sypula, M., and Synthesis, M.G. *Supramol. Chem* 2010, *22,* 827.
21. Lee, C., Yang, W., and Parr, R.G. Development of the Colle-Salvetti correlation-energy formula into a functional of the electron density *Phys. Rev. B* 1988, *37,* 785.
22. Weigend, F. and Ahlrichs, R. Balanced basis sets of split valence, triple zeta valence and quadruple zeta valence quality for H to Rn: Design and assessment of accuracy *Phys. Chem. Chem. Phys.* 2005, *7,* 3297.
23. TURBOMOLE V7.0, a development of University of Karlsruhe and Forschungszentrum KarlsruheGmbH, 1989–2007; TURBOMOLE GmbH, since 2007. http://www.turbomole.com.
24. Küchle, W., Dolg, M., Stoll, H., and Preuss, H. Energy-adjusted pseudopotentials for the actinides. Parameter sets and test calculations for thorium and thorium monoxide *J. Chem. Phys.* 1994, *100,* 7535.
25. Ishimori, K., Watanabe, M., Kimura, T., Yaita, T., Yamada, T., Kataoka, Y., Shinoda, S., and Tsukube, H. Novel separation system of trivalent actinides — combined effects of substituted tris(2-pyridylmethyl)amine ligand and hydrophobic counter-anion *Chem. Lett.* 2005, *34,* 1112.
26. Lemaire, M., Guy, A., Chomel, R., and Foos, J. Dicyclohexano-18-crown-6 ether: a new selective extractant for nuclear fuel reprocessing *J. Chem. Soc., Chem. Commun.* 1991, 1152.
27. Tsaryuk, V.I., Savchenko, V.D., Aryutkina, N.L., and Chenskaya, T.B. Vibronic spectra of europium nitrate hexahydrate *J. Appl. Spectrosc.* 1994, *60,* 185.
28. Tsaryuk, V.I., Savchenko, V.D., Zolin, V.F., and Kudryashova, V.A. Vibronic interaction in europium nitrates $Eu(NO_3)_3 \cdot 4SOR_2$ *Spectrochimica Acta A* 2000, *56,* 1149.
29. Steppert, M., Cisarova, I., Fanghänel, T., Geist, A., Lindqvist-Reis, P., Panak, P., Stepnicka, P., Trumm, S., and Walther, C. Complexation of europium(III) by bis(dialkyltriazinyl)bipyridines in 1-octanol *Inorg. Chem.* 2012, *51,* 591.
30. Chodos, S.L. and Satten, R.A. Model calculation of vibronic sidebands in Cs_2UBr_6 *J. Chem. Phys.* 1975, *62,* 2411.
31. Iben, I.E., Stavola, M., Macgregor, R.B., Zhang, X.Y., and Friedman, J.M. Gd^{3+} vibronic side band spectroscopy. New optical probe of Ca^{2+} binding sites applied to biological macromolecules *Biophys. J.* 1991, *59,* 1040.